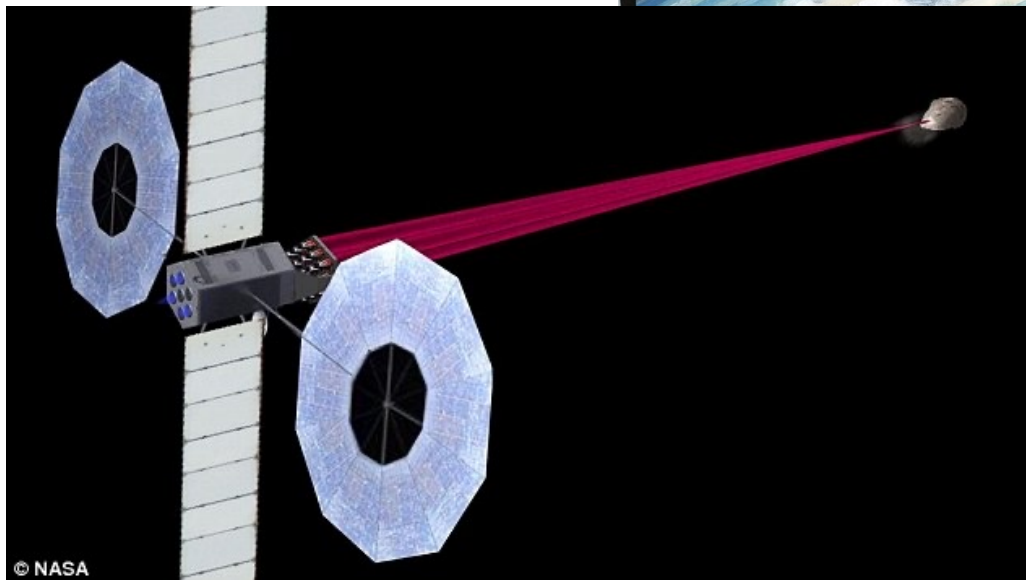


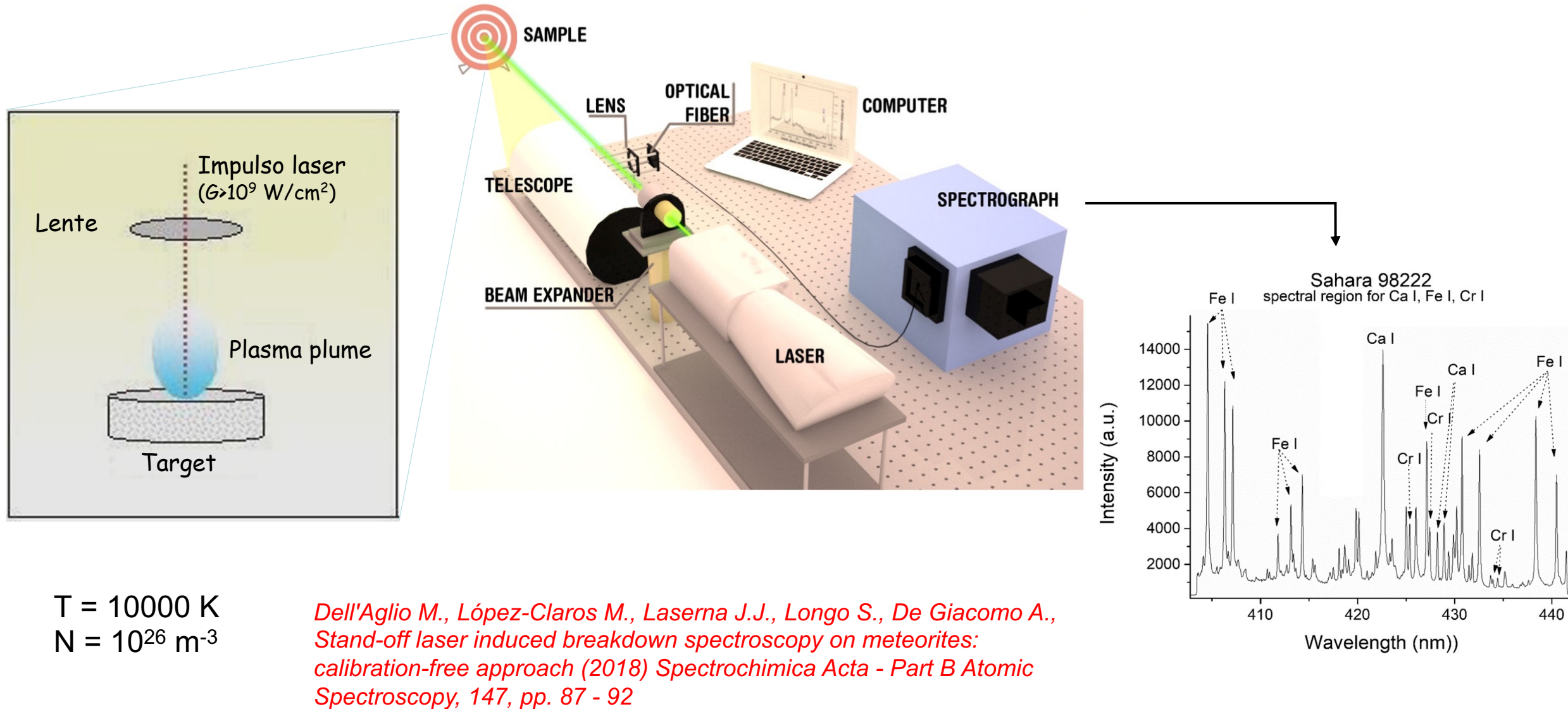
*Il contributo dell'analisi chimica con
tecniche laser per l'esplorazione dello
spazio e della terra*

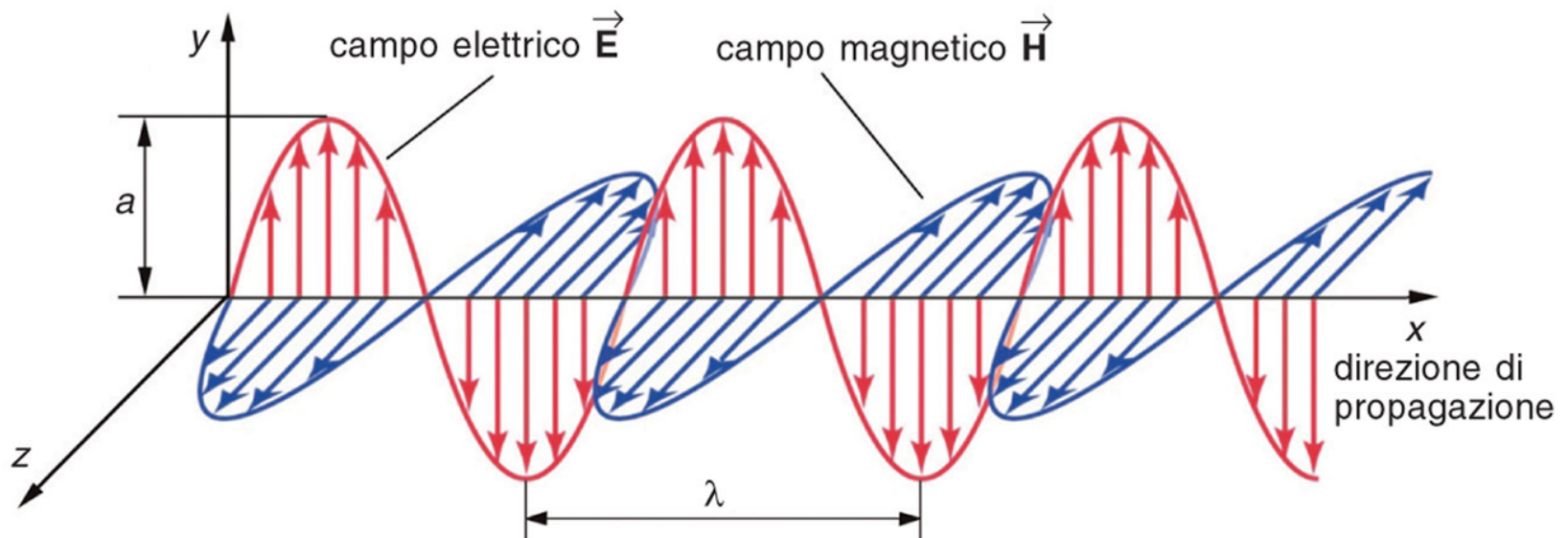
Prof. Alessandro De Giacomo

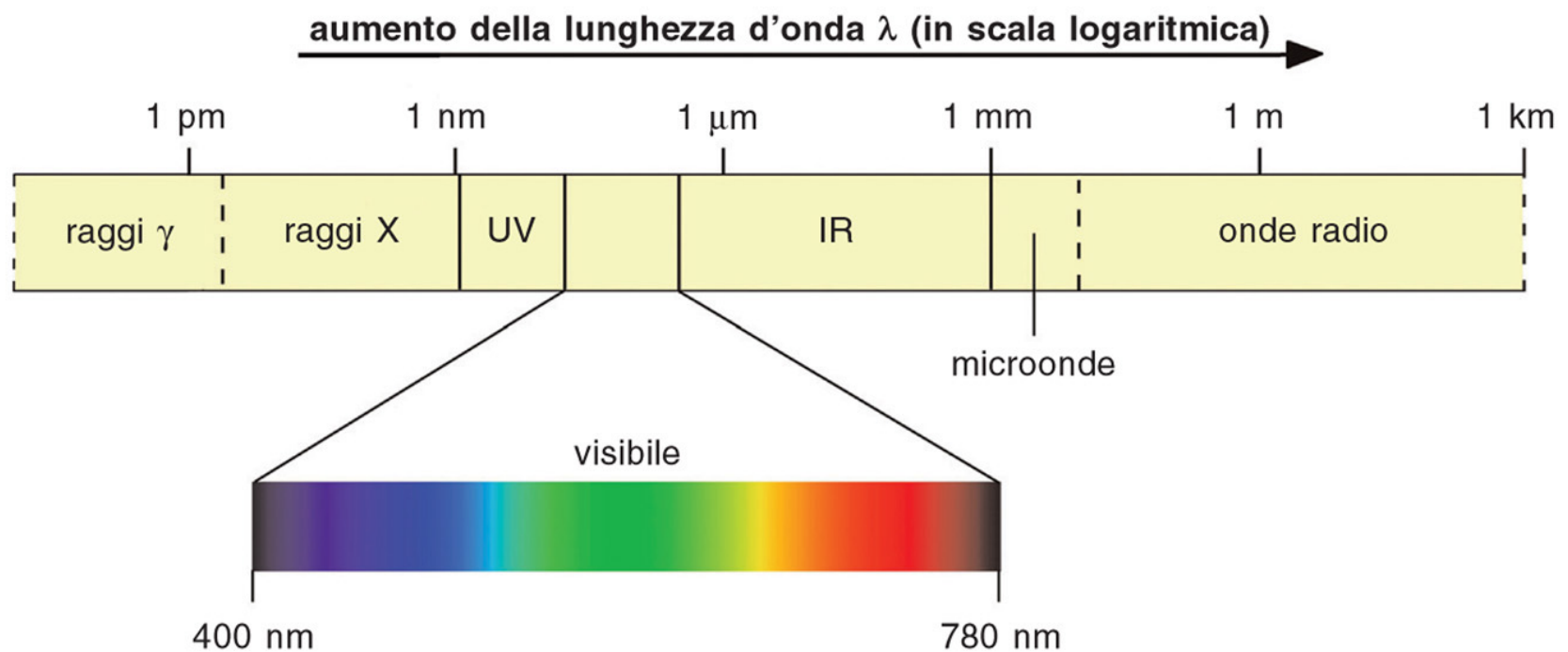


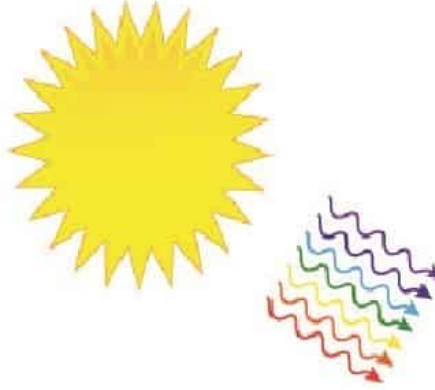
LIBS

Laser Induced Breakdown Spectroscopy

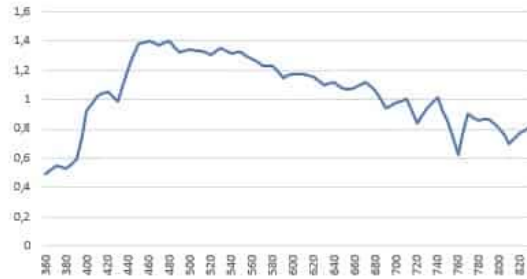




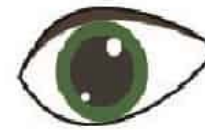
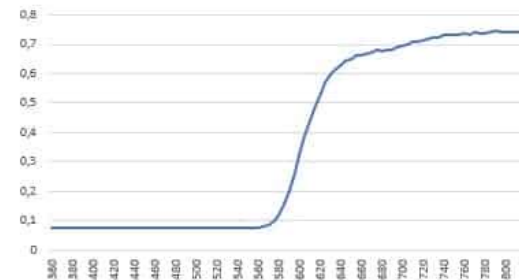




Spettro sorgente

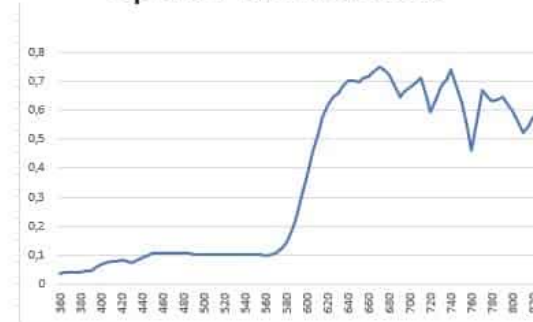


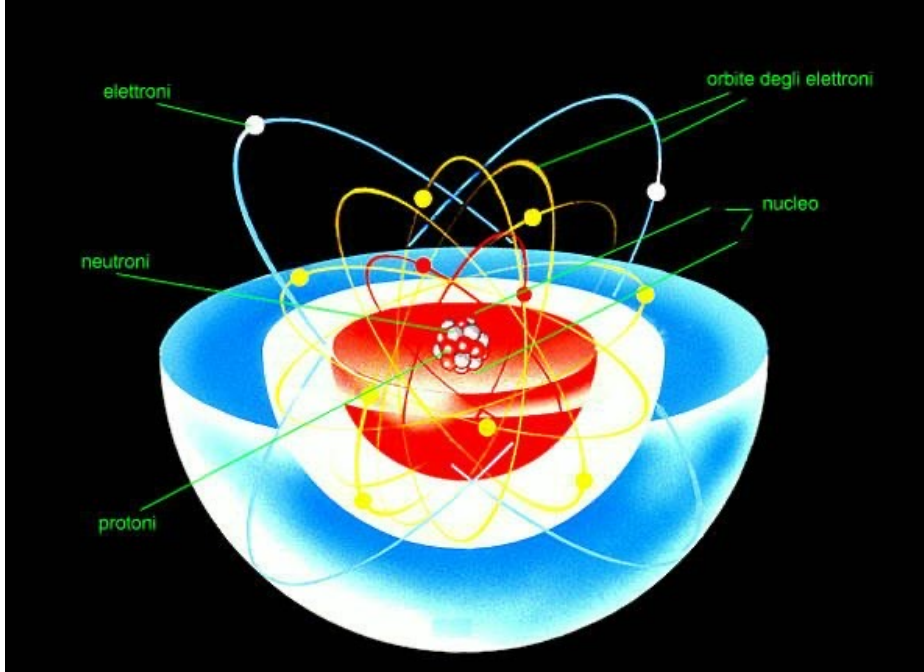
Riflettanza oggetto



ROSSO

Spettro luce riflessa

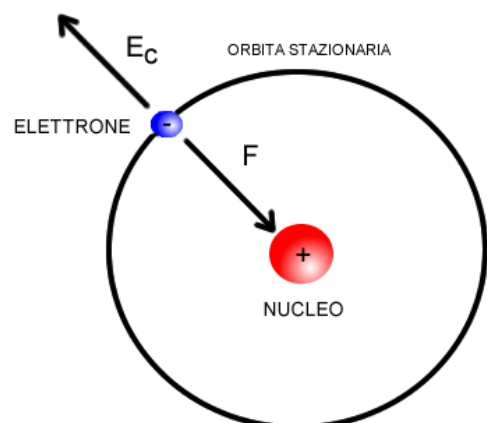




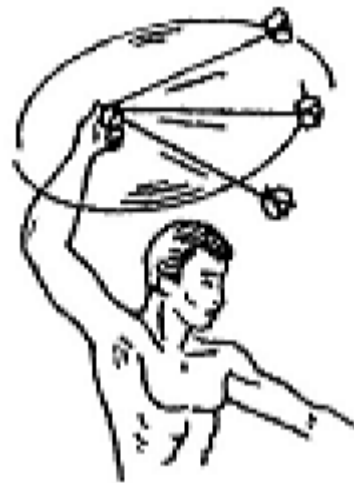
Massa del protone = $1,67262171 \times 10^{-27}$ kg

Massa del neutrone = $1,67492729 \times 10^{-27}$ kg

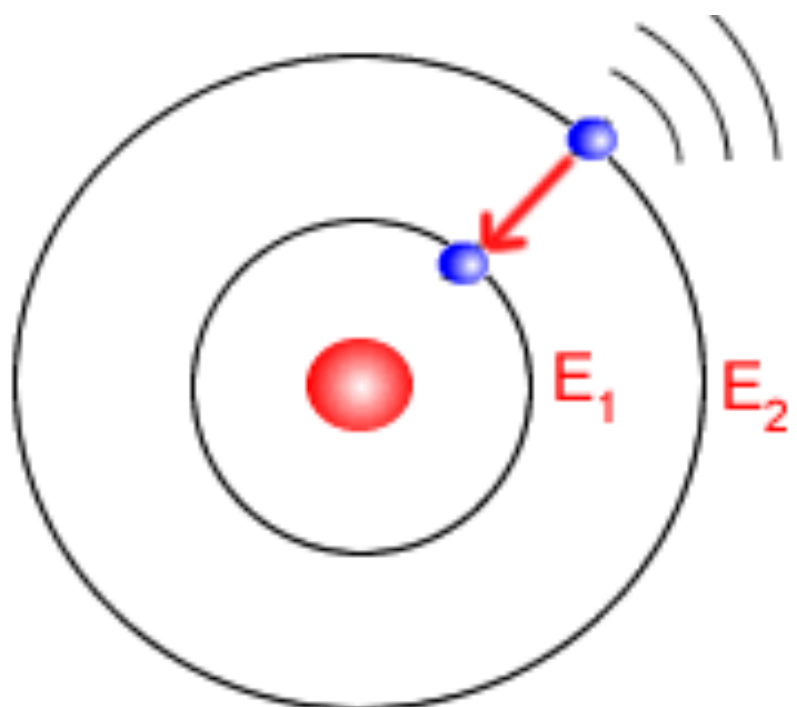
Massa dell'elettrone = $9.1093826 \times 10^{-31}$ kg



ORBITA STAZIONARIA

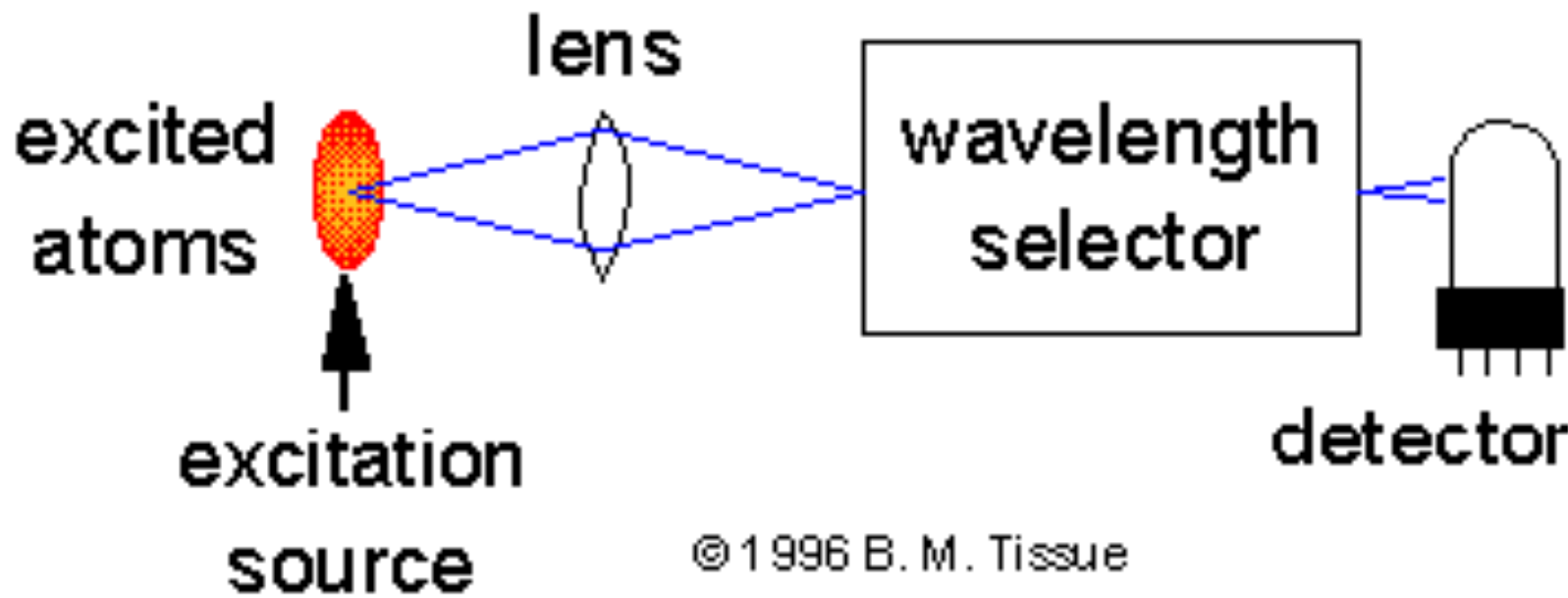
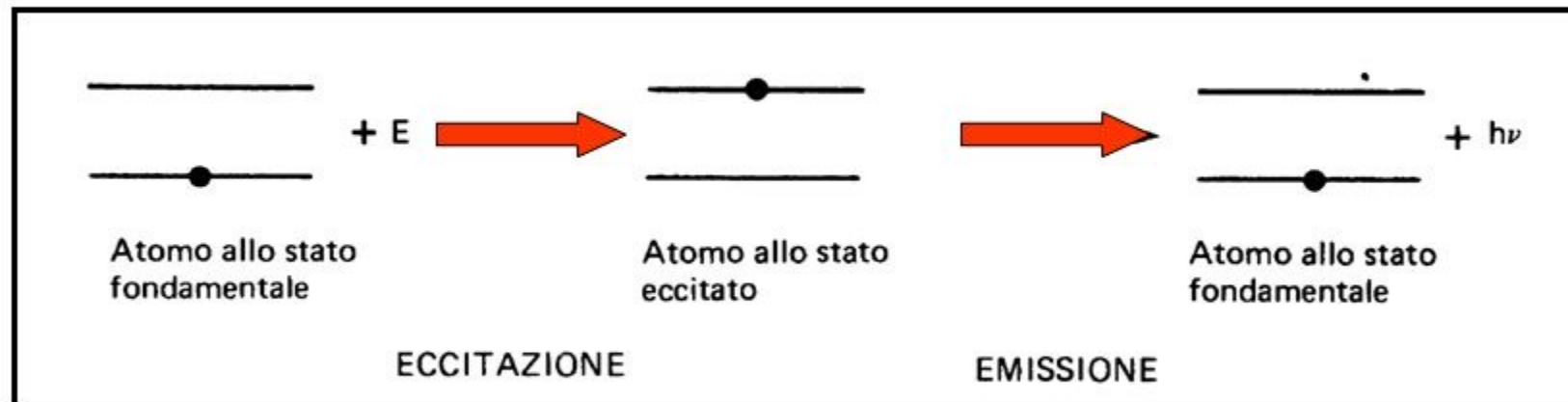


WWW.ANDREAMININI.ORG

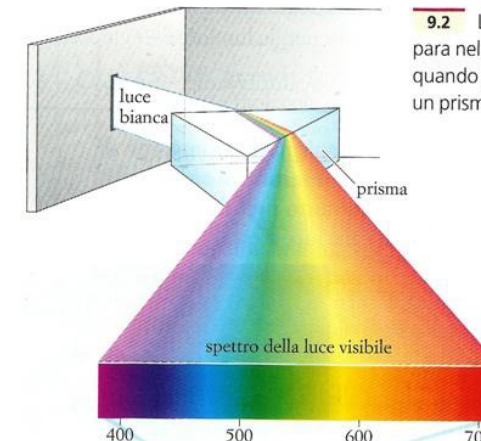
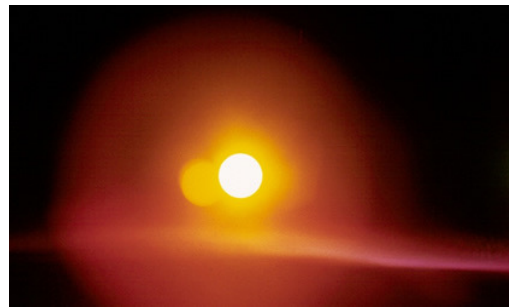


$$E_2 - E_1 = h\nu$$

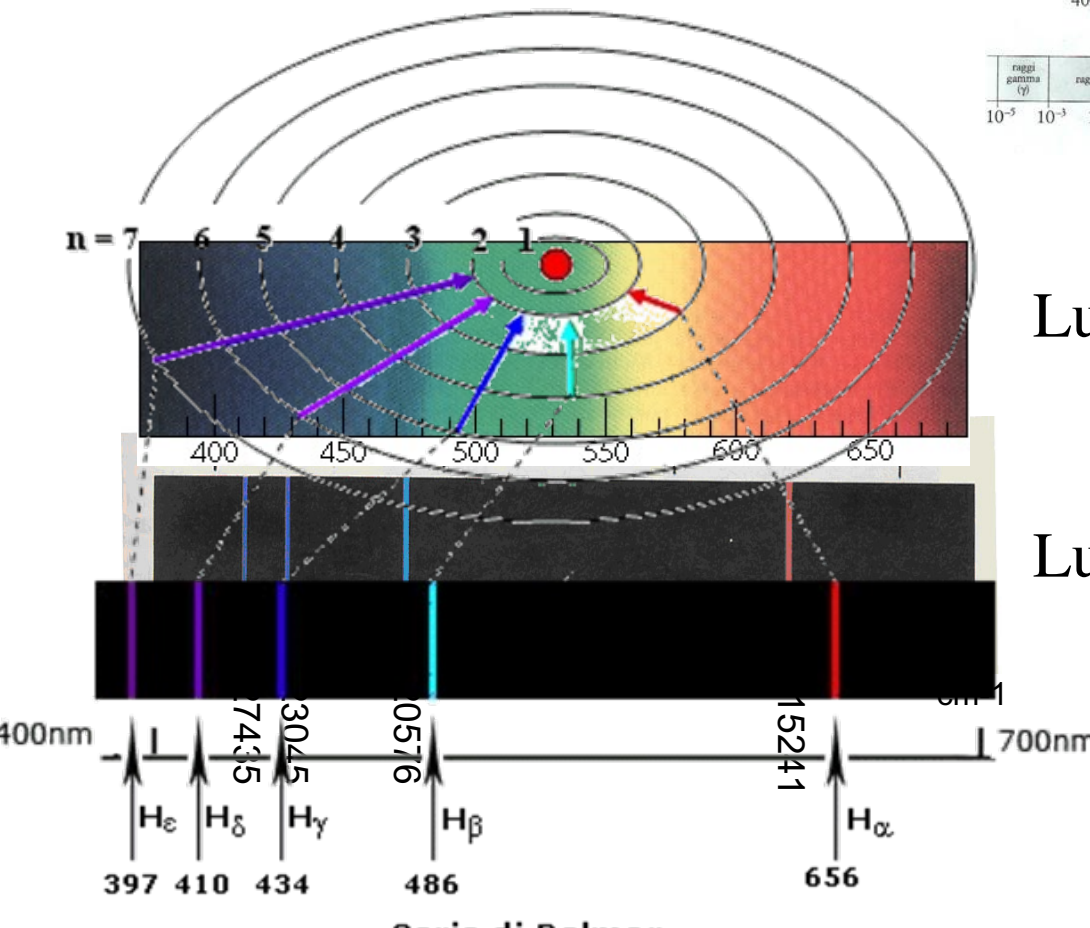
Spettroscopia di emissione atomica



© 1996 B. M. Tissue



9.2 La luce bianca si separa nelle sue componenti quando passa attraverso un prisma.



Luce bianca

Luce emessa dall' H

Problematiche dell'analisi elementare in ambienti ostili



1) Calibrazione strumentale

Stabilità e riproducibilità condizioni sperimentali
e cammino ottico

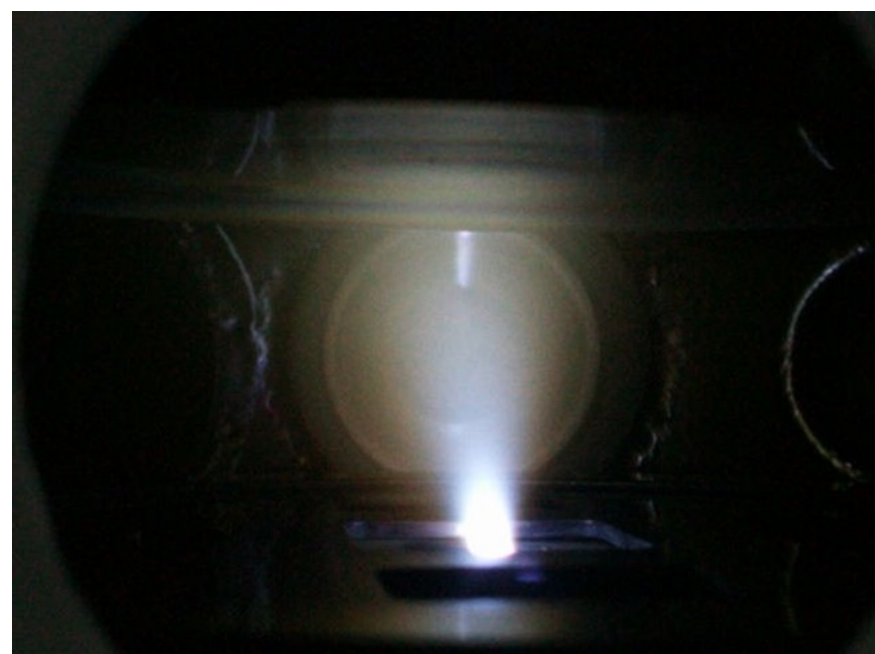
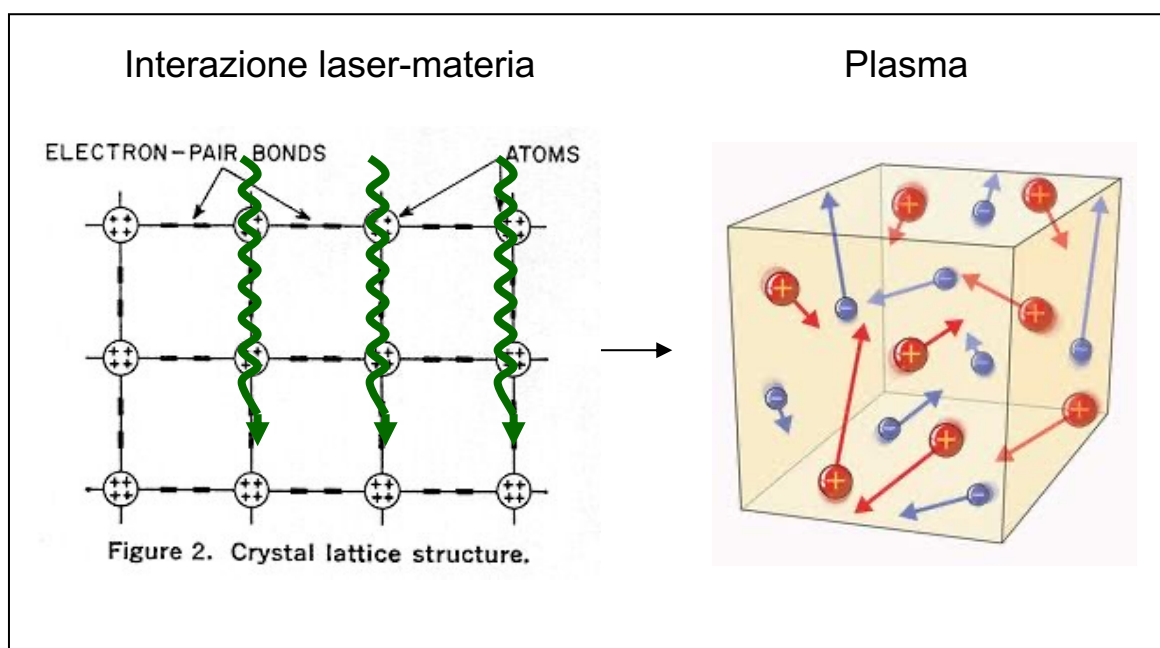
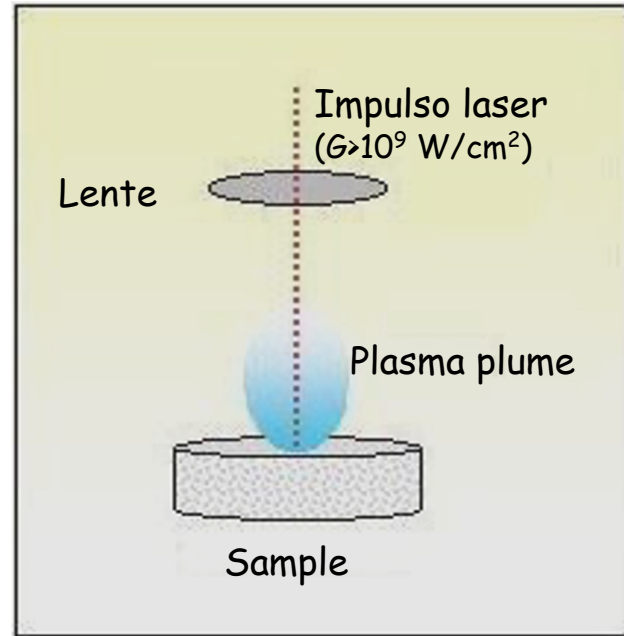
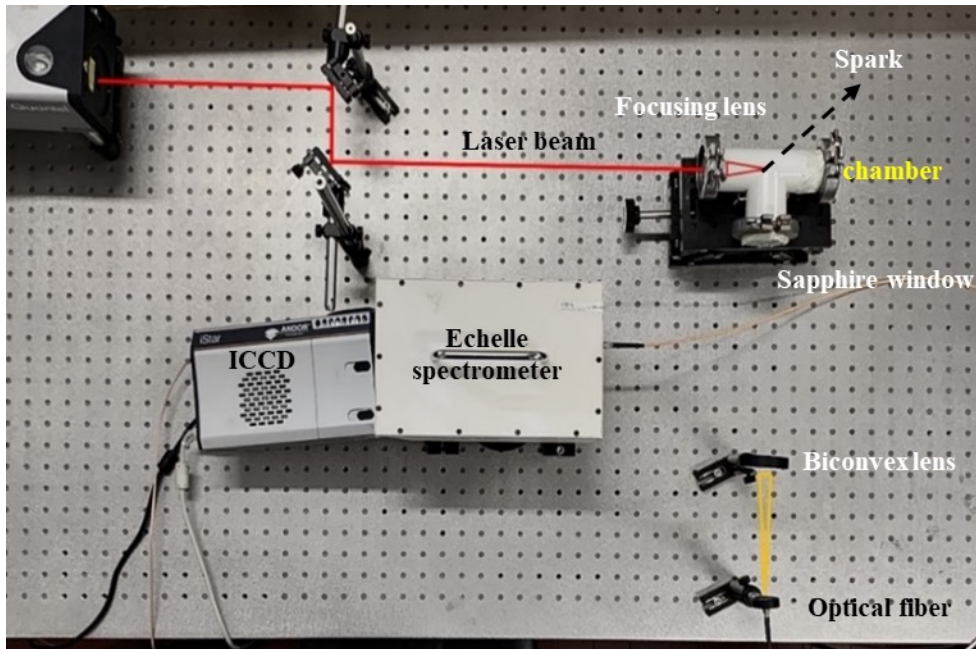
2) Matrix match standards

Standard con matrici simili al campione

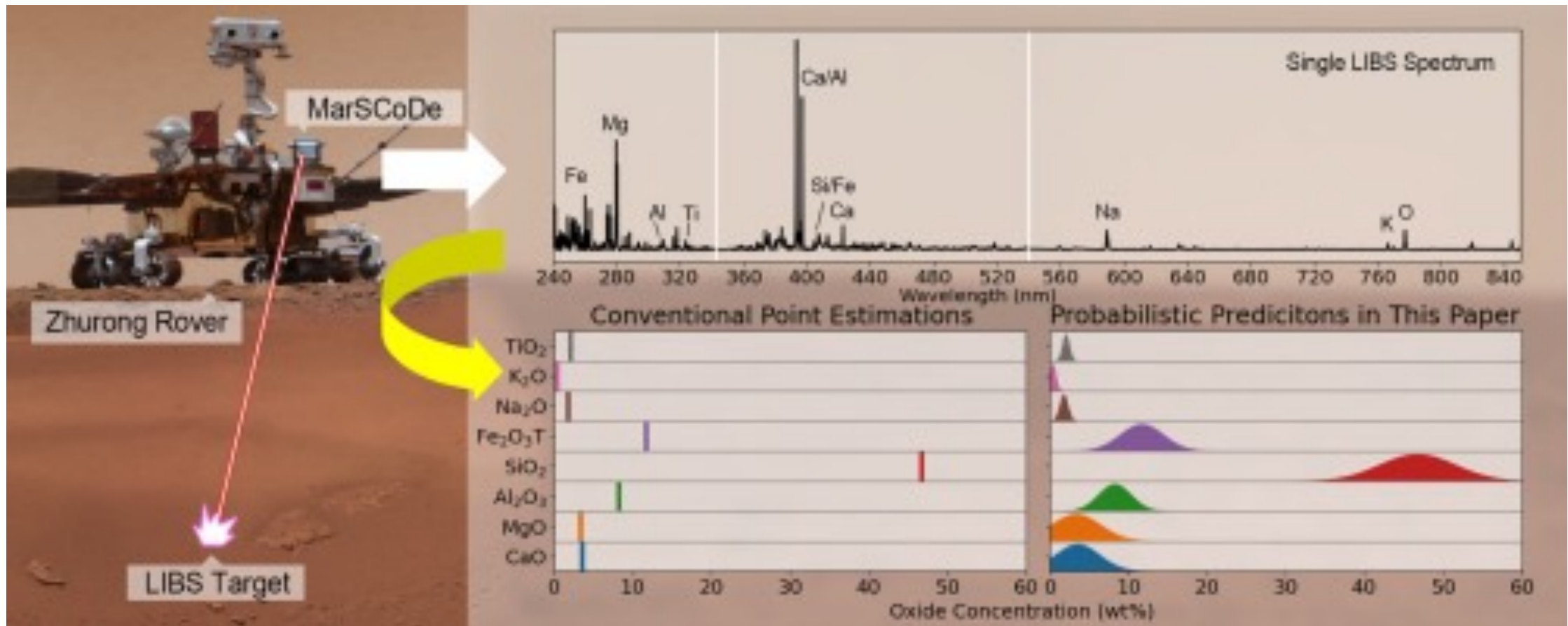
3) Curve di calibrazione

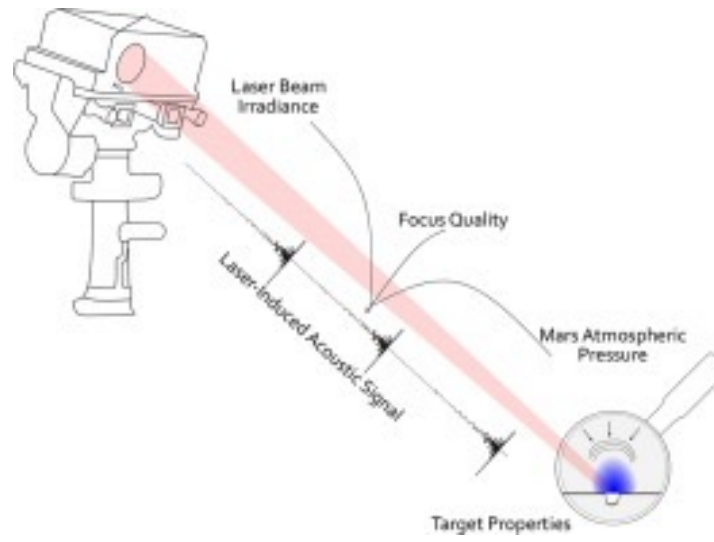
Quantità di campione nota e riproducibile

IMPOSSIBILE



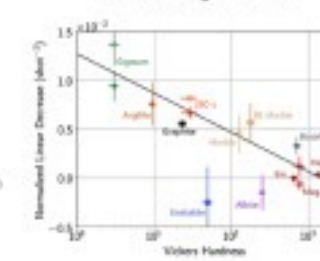
Esplorazione di Marte



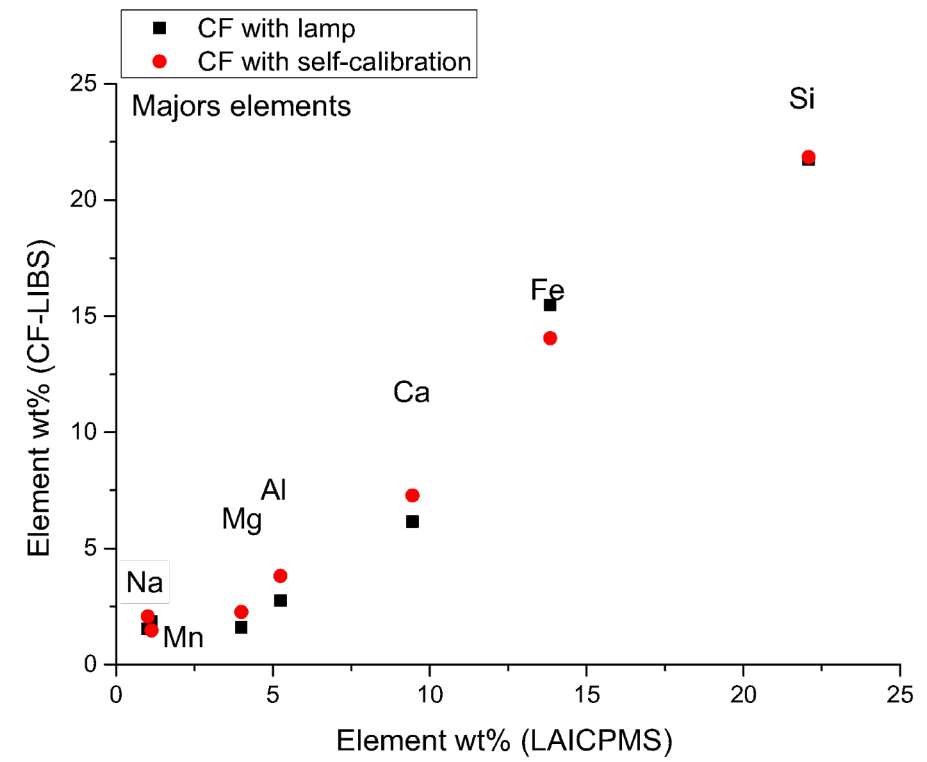
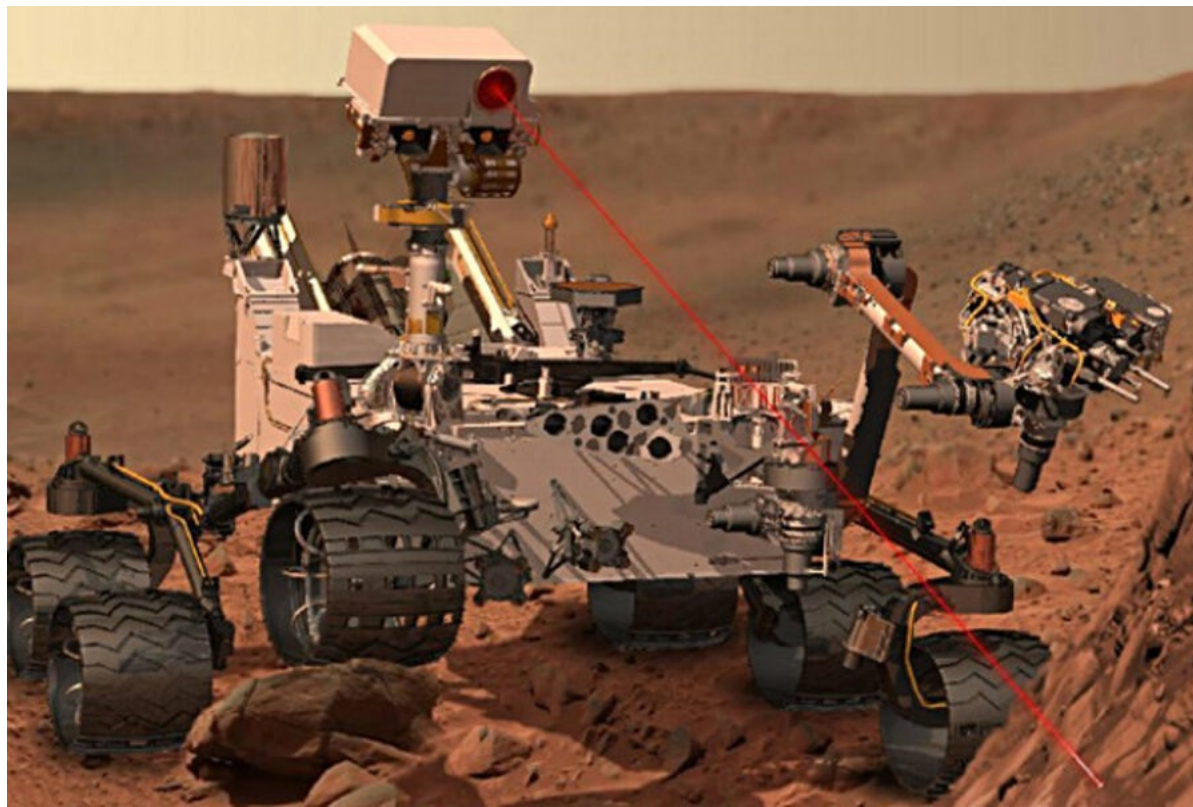
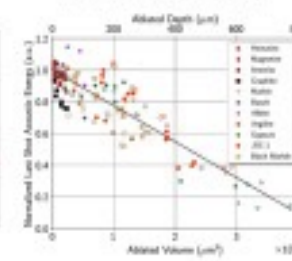


Recording Laser-Induced Sparks on Mars to...

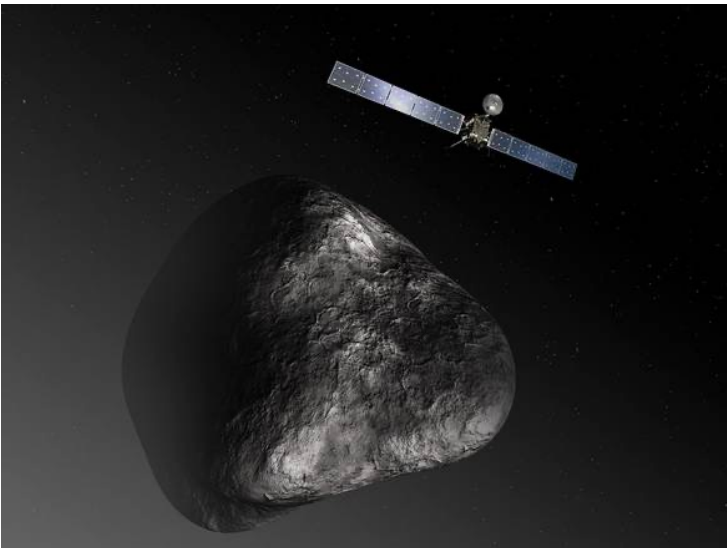
Estimate target hardness



Measure ablated volume



LIBS and Space Exploration

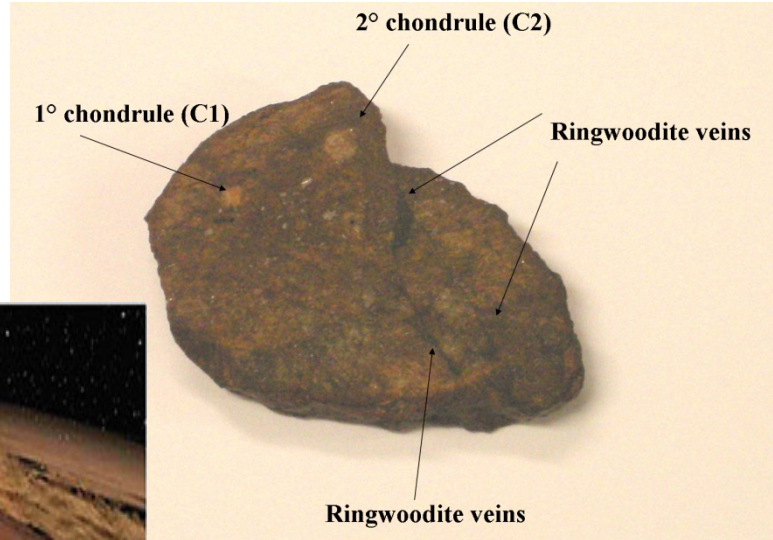
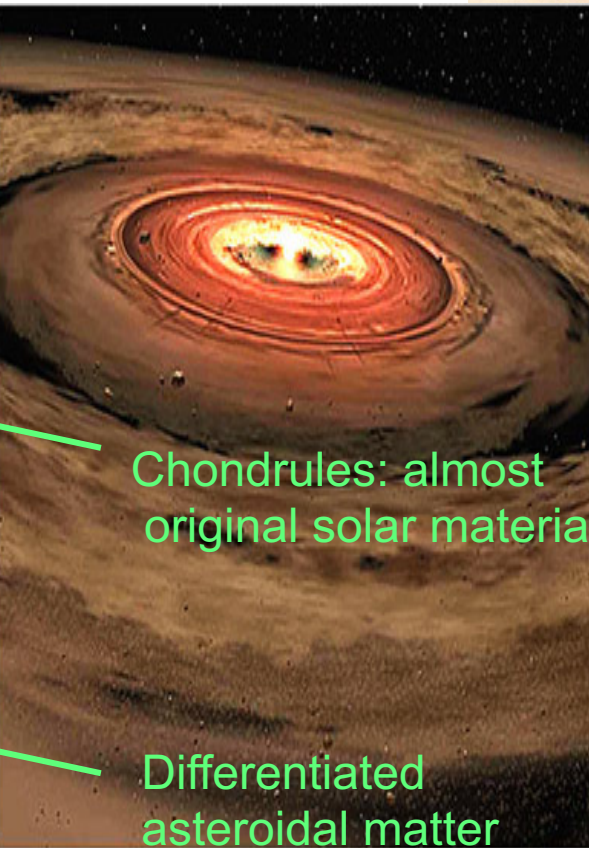
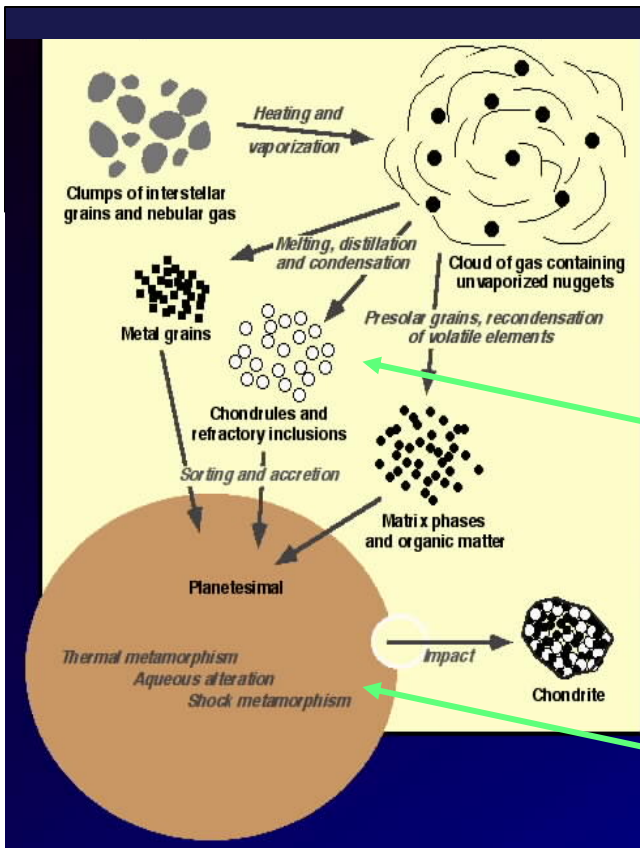


Asteroids, comets and meteorites

PON “Apulia Space” (PON03PE_00067_6)

LIBS on meteorites as a probe of the early solar system

First test case: chemical composition of chondrites and chondrules



2.6. Iron alloys analysis: iron meteorites

Sikhote Alin



Toluca



Campo del cielo



	CF (50 ns)			Literature			CF (5000 ns)		
	Fe	Ni	Co	Fe	Ni	Co	Fe	Ni	Co
Sikote Alin	93.0	6.3	0.8	93.5	6.0	0.48	94.0	5.7	0.6
Toluca	92.3	6.9	0.8	91.5	8.2	0.45	92.0	7.1	0.35
Campo del Cielo	93.1	6.2	0.5	92.6	6.9	0.50	91.0	8.0	0.7

Chemical elemental analysis

wt %	<i>Dhofar 019</i>		<i>Dhofar 461</i>		<i>Sahara 98222</i>	
	LIBS	Literature ²	LIBS	Literature ³	LIBS	Literature ⁴
Al	1.4 ± 0.2	3.40	14 ± 1	15.50	0.88 ± 0.09	1.22
Ti	0.45 ± 0.06	0.37	0.25 ± 0.04	0.13	0.060 ± 0.009	0.063
Mg	9.5 ± 0.9	8.80	1.5 ± 0.2	2.40	13 ± 1	14.9
Mn	0.35 ± 0.04	0.38	0.050 ± 0.005	0.05	0.26 ± 0.03	0.257
Cr	0.6 ± 0.1	0.40	-	-	0.95 ± 0.09	0.388
Ca	3.6 ± 0.6	5.20	12 ± 1	11.90	1.0 ± 0.1	1.31
Fe	17 ± 2	14.70	4.9 ± 0.5	3.17	21 ± 2	21.5
Si	24 ± 2	22.62	22 ± 2	21.00	20 ± 2	18.5
Ni	-	-	-	-	0.22 ± 0.02	1.2
Co	-	-	-	-	0.014 ± 0.002	
O_{calc}	42 ± 6	44.20	44 ± 5	45.00	39 ± 4	37.7

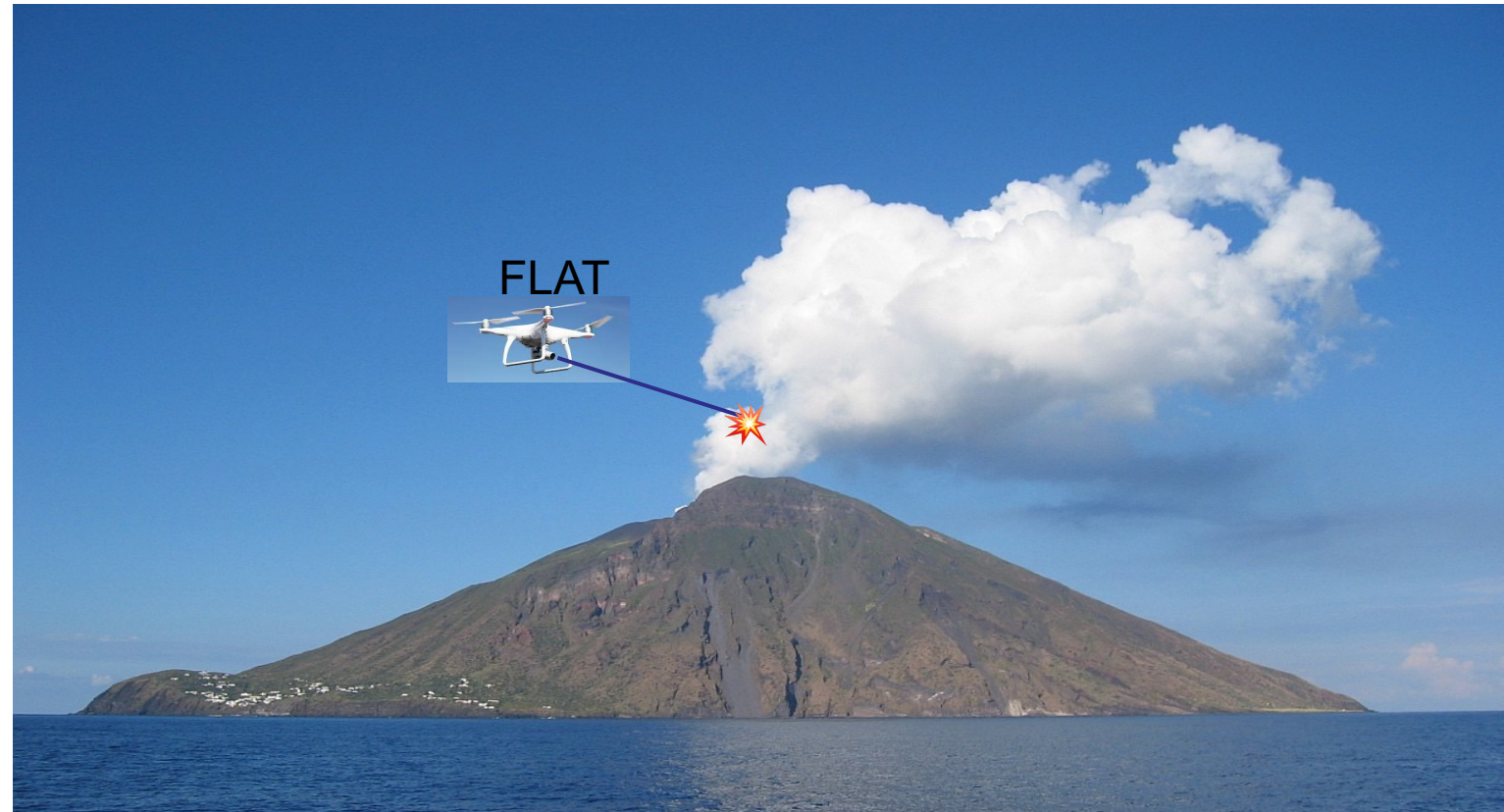
²Taylor et al., 2002

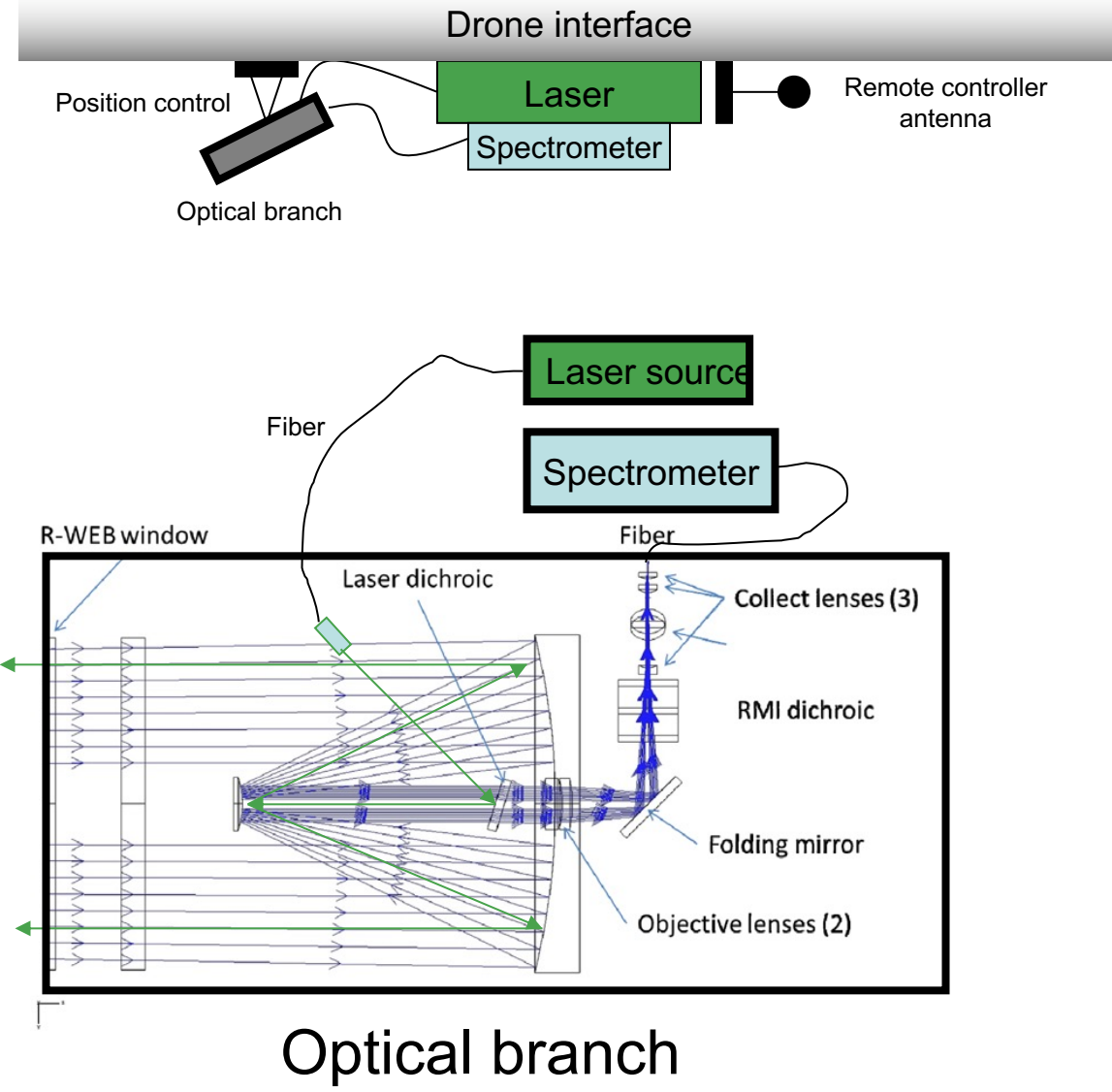
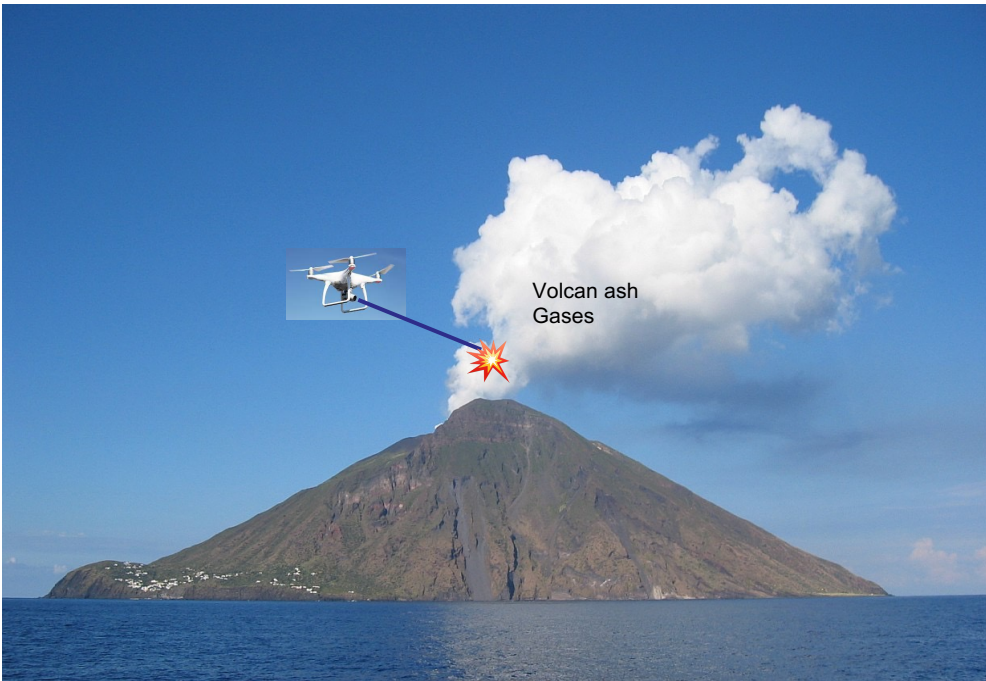
³Wasson et al., 1988

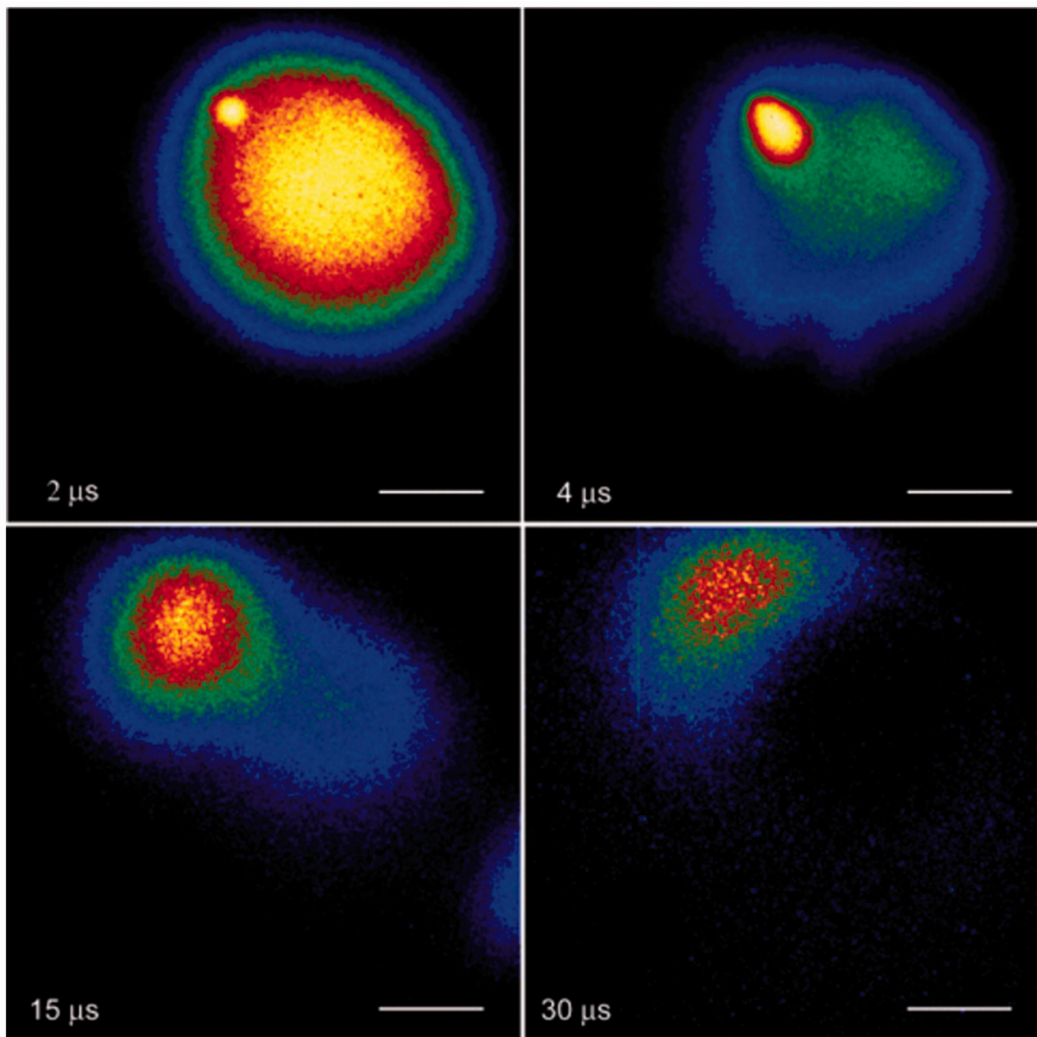
²Wasson et al., 2007
³Wasson et al., 2002

wt %	<i>Sikhote Alin</i>		<i>Campo del Cielo</i>		<i>Toluca</i>	
	LIBS	Literature ²	LIBS	Literature ³	LIBS	Literature ³
Fe	94 ± 13	93.49	91 ± 14	92.61	92 ± 13	91.49
Ni	5.7 ± 0.6	6.03	8 ± 1	6.94	7.1 ± 0.8	8.02
Co	0.6 ± 0.1	0.48	0.7 ± 0.1	0.45	0.34 ± 0.07	0.49

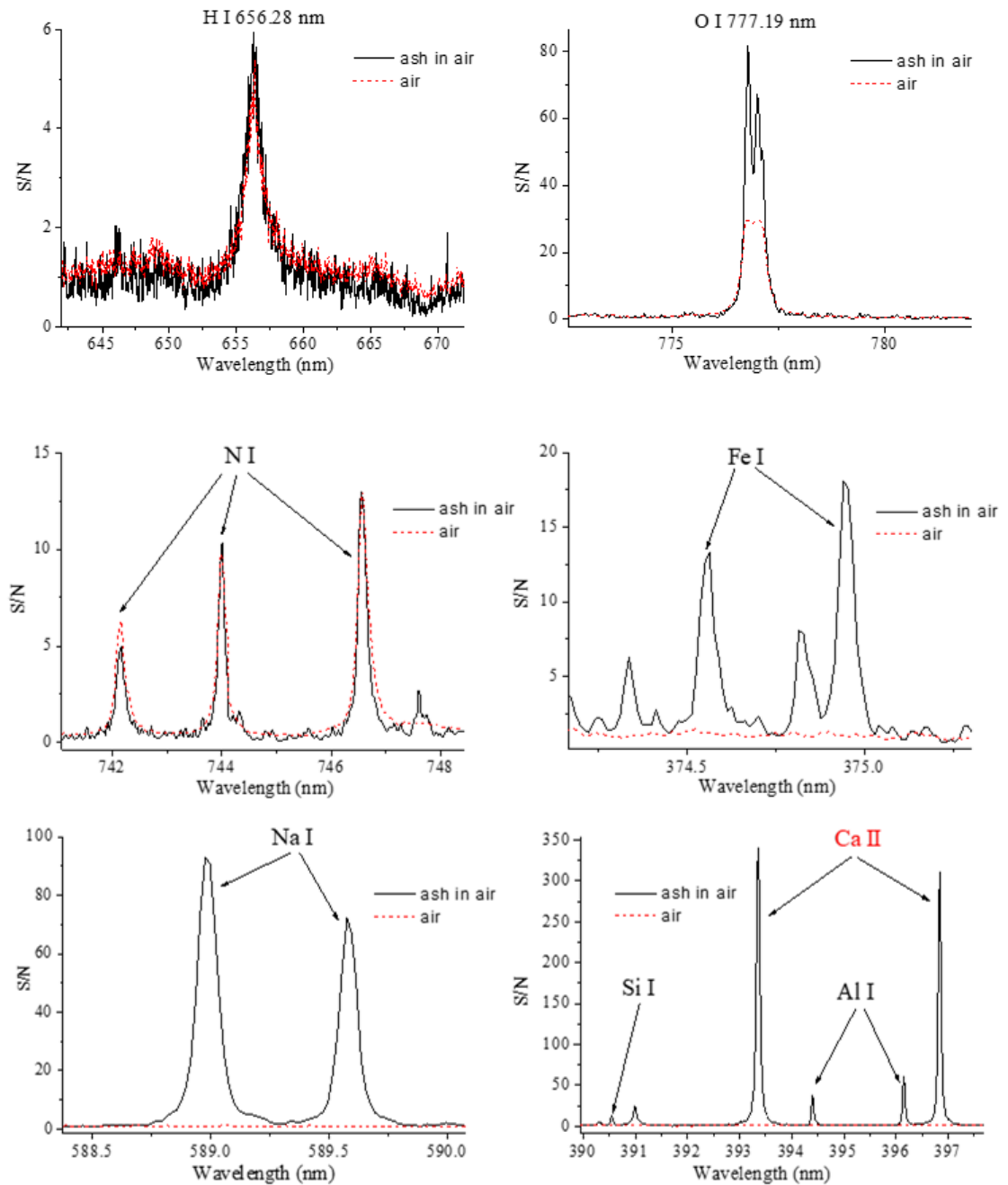
Monitoraggio Plume vulcanici







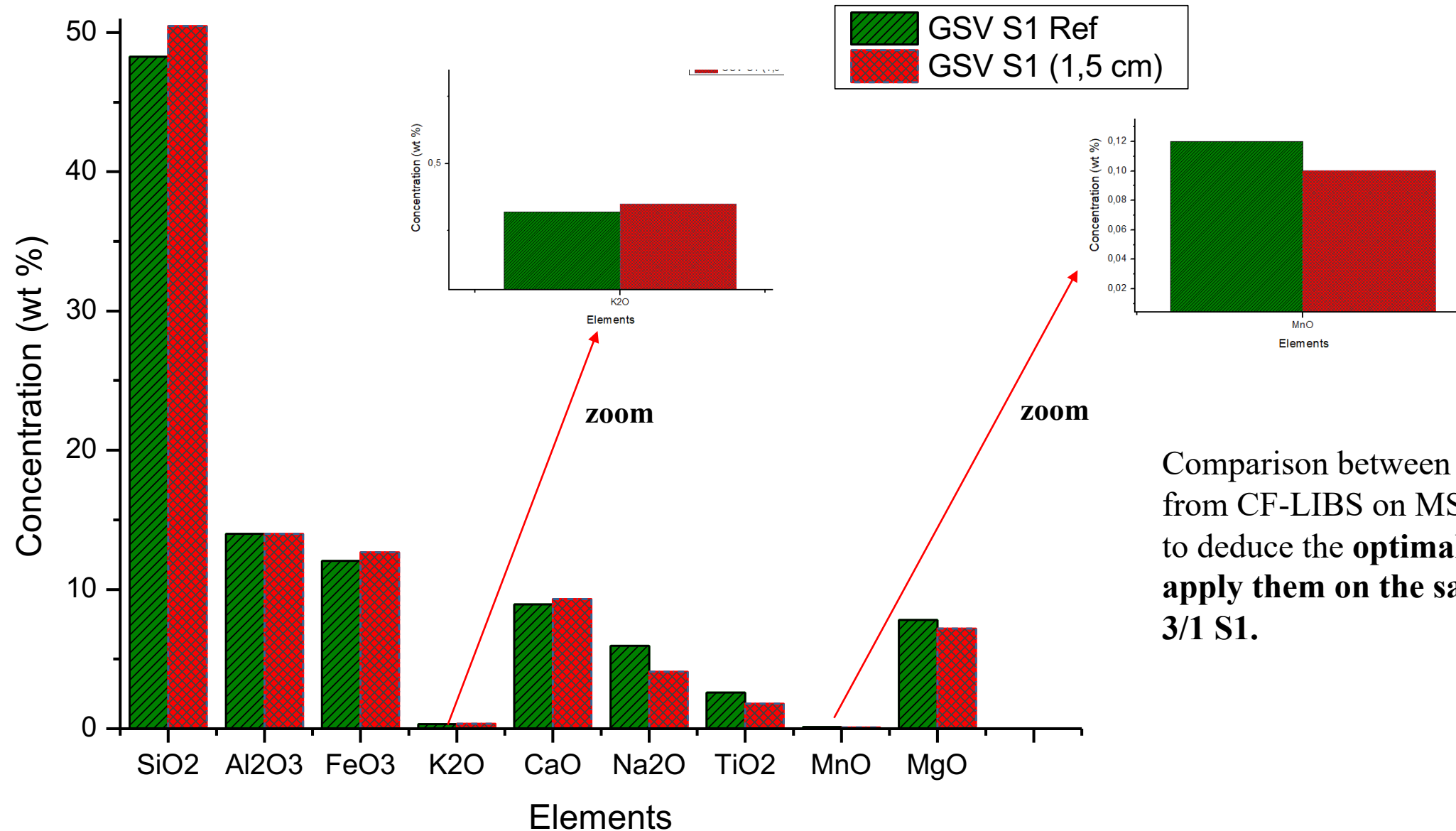
Hohreiter V., Hahn D.W. "Plasma-Particle Interactions in a Laser-Induced Plasma: Implications for Laser-Induced Breakdown Spectroscopy". *Anal. Chem.* 2006; 78(5): 1509–1514



Volcanic ash analysis

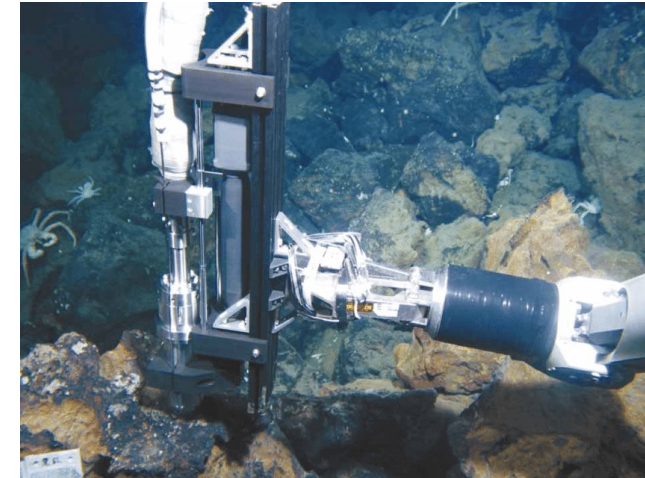
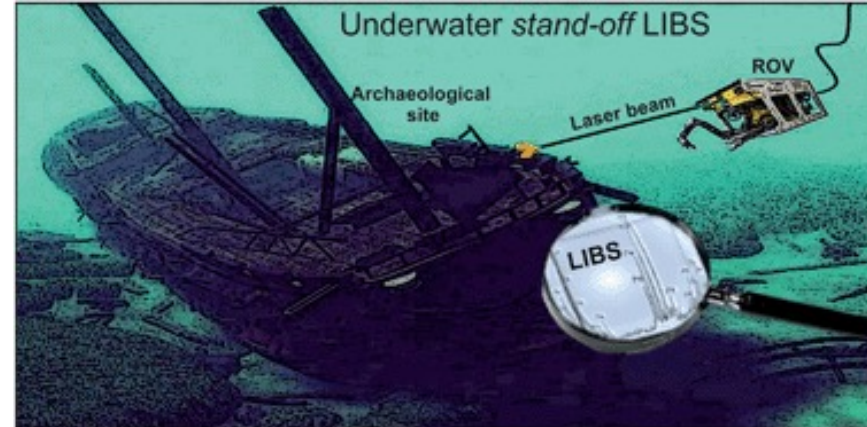
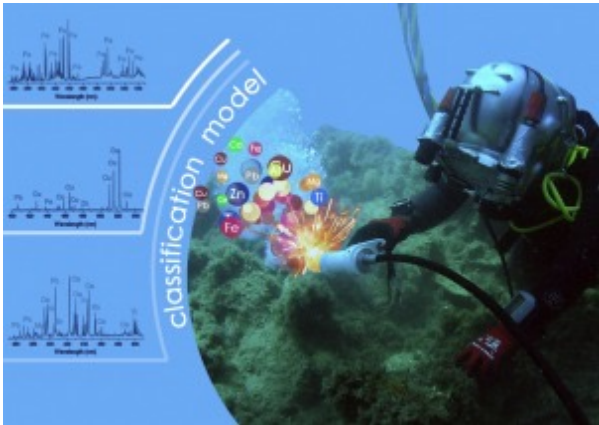
Calibration-Free Laser Induced Breakdown Spectroscopy : GSV 3/1 S1

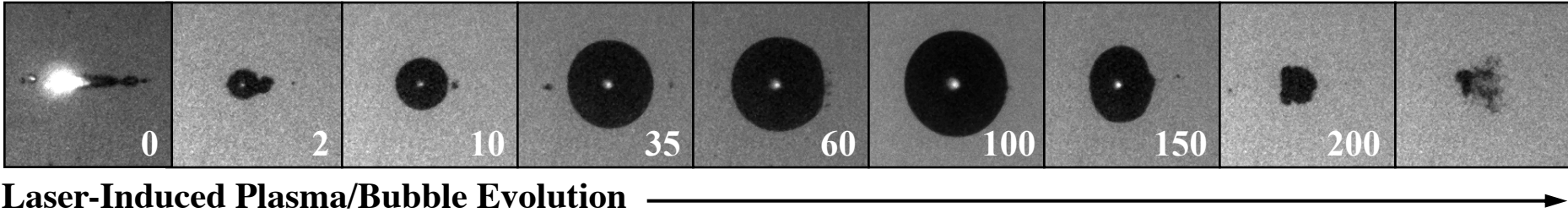
Distance between the laser pulse and the sample **1,5 cm** and laser energy **150 mJ**



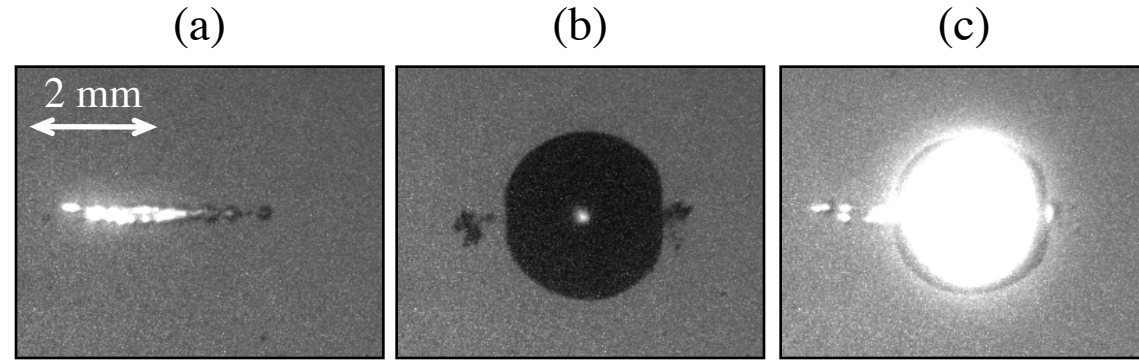
Comparison between the results obtained from CF-LIBS on MS 151/6 ash allowed to deduce the **optimal conditions and apply them on the same size ash GSV 3/1 S1.**

Esplorazione del mare





Evolution of the laser-induced bubble formed in bulk aqueous solution ($P = 1$ bar) using a single laser pulse ($E1 = 7$ mJ/pulse) incident from the left of the images. For all images, $td = 800$ ns, $tb = 1$ μ s, and $P = 1$ bar. The delay following the laser-pulse, Δt , was varied and is indicated in the bottom right-hand corner of each image. The bubble had a maximum radius of approximately 2.5 mm ($\Delta t = 100$ μ s). Each shadowgram corresponds to 4 x 4 mm region around the focal volume. The bright spot in the middle of the bubble ($2 \leq \Delta t \leq 150$ μ s) is transmitted light from the background illumination source (not plasma emission).



Shadowgraph images of (a) SP-LIBS plasma, using $E2$ only; (b) laser-induced bubble, using $E1$ only, $\Delta t = 60$ μ s; and (c) DP-LIBS plasma, using $E1$ and $E2$, $\Delta t = 60$ μ s. $E1 = 7$ mJ/pulse and $E2 = 30$ mJ/pulse. For all images, $td = 800$ ns, $tb = 1$ μ s, and $P = 1$ bar. The laser pulse was incident from the left of the images. Each shadowgram corresponds to 4 x 5 mm region around the focal volume. The bright spot in the middle of the bubble in (b) is transmitted light from the background illumination source (not plasma emission).

<https://youtu.be/fEZ5dEi4oPo>